

See discussions, stats, and author profiles for this publication at: <https://www.researchgate.net/publication/51123012>

# Properties of Chlorophyll and Derivatives in Homogeneous and Microheterogeneous Systems

ARTICLE *in* THE JOURNAL OF PHYSICAL CHEMISTRY B · JUNE 2011

Impact Factor: 3.3 · DOI: 10.1021/jp201278b · Source: PubMed

CITATIONS

11

READS

28

6 AUTHORS, INCLUDING:



**Tayana Mazin Tsubone**

University of São Paulo

6 PUBLICATIONS 31 CITATIONS

SEE PROFILE



**Hueder Paulo Moisés De Oliveira**

Universidade Federal do ABC (UFABC)

42 PUBLICATIONS 392 CITATIONS

SEE PROFILE



**Noboru Hioka**

Universidade Estadual de Maringá

71 PUBLICATIONS 718 CITATIONS

SEE PROFILE



**Wilker Caetano**

Universidade Estadual de Maringá

53 PUBLICATIONS 617 CITATIONS

SEE PROFILE

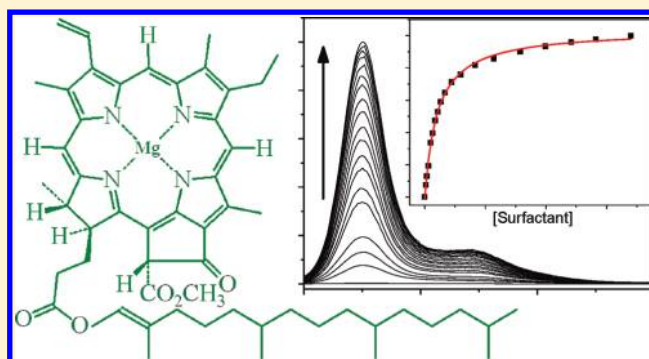
# Properties of Chlorophyll and Derivatives in Homogeneous and Microheterogeneous Systems

Adriana P. Gerola,<sup>†</sup> Tayana M. Tsubone,<sup>†</sup> Amanda Santana,<sup>†</sup> Hueder P. M. de Oliveira,<sup>‡</sup> Noboru Hioka,<sup>†</sup> and Wilker Caetano<sup>\*,†</sup>

<sup>†</sup>Chemistry Department, State University of Maringá, Av. Colombo, 5790, Paraná, Brazil 87020-900

<sup>‡</sup>Federal University of Pelotas, Pelotas, Rio Grande do Sul, Brazil

**ABSTRACT:** Chlorophyll (Mg-Chl) and its derivatives, zinc chlorophyll (Zn-Chl), copper chlorophyll (Cu-Chl), pheophytin (Pheo), pheophorbide (Pheid), and zinc chlorophyllide (Zn-Chld), were studied as to their acid–base equilibrium properties, hydrophobicity, stability, binding, and relative localization in neutral surfactant micellar systems. The stability order of metalochlorophyll ( $pH_M$ ) in acidic medium was found to be Cu-Chl > Zn-Chld > Zn-Chl > Mg-Chl. The apparent  $pK_a$  for protonation of porphyrin ring nitrogens was around 1.0 for all derivatives. The  $pK_a$  for protonation of carboxylate phorbide was 5.9 for Pheid and 2.4 for Zn-Chld. This difference was attributed to complexation of carboxylate with zinc. The hydrophobicity of chlorophyll in relation to the ability of partitioning the cell membrane lipid layer was estimated in the octanol/water biphasic system. Pheo, a more hydrophobic molecule, presented the highest partition coefficient ( $K_p$ ) in the organic phase, followed by Cu-Chl, Mg-Chl, Zn-Chl, Pheid, and Zn-Chld. The hydrophobic character was the key to relative drug location in the micellar systems. All studied derivatives interacted strongly with Tween 80 micellar systems, and particularly with P-123. For both surfactants, the order followed by binding constant ( $K_b$ ) was Zn-Chld > Pheo > Cu-Chl > Mg-Chl > Zn-Chl > Pheid, while binding constants estimated for the Chl containing the phytol group correlated with  $K_p$ . Fluorescence quenching studies have shown that phorbides are located in a less hydrophobic region than the phytol chain-containing derivatives, which are located preferentially in a deeper micellar microenvironment. Thus, the association of the chlorophylls with specific binding sites of micellar systems is strongly modulated by the presence of phytol chains and metal coordinated to the porphyrinic ring.



## INTRODUCTION

Chlorophylls (Chl) are a class of molecules found in abundance in nature and are fundamental in the photosynthesis processes, together with other pigments like carotenoids and bacteriochlorophylls. Chl acts in photon capturing and excitation energy transfer and storage in the antennae in reaction centers (RC) in photosystems I and II.<sup>1,2</sup> The interaction of Chl with apoproteins changes the  $\pi$ -electron system, leading to variations in redox potential and spectral properties of these compounds and functional versatility as photosynthetic cofactors.<sup>3–9</sup>

The molecular structure of chlorophyll is a porphyrin ring with one reduced pyrrole ring (chlorine-type compound) with a  $Mg^{2+}$  ion coordinated to nitrogens and a long nonpolar phytic chain, which enhances the hydrophobicity of the molecule as shown to chlorophyll *a* derivatives in Figure 1. The substitution of  $Mg^{2+}$  ion in the tetrapyrrole ring of chlorophyll by hydrogen atoms results in pheophytin (Pheo), which presents a more hydrophobic character than its precursor.<sup>10</sup> Chlorophylls complexed with the divalent cations  $Zn^{2+}$  and  $Cu^{2+}$ , known as transmetalated chlorophylls, are termed chlorophyll zinc (Zn-Chl) and copper (Cu-Chl), respectively. The Zn and Cu chlorophylls present high stability in

Chls	Ligand (L)	Residue (R)
Mg-Chl	Mg	Phytol
Zn-Chl	Zn	Phytol
Cu-Chl	Cu	Phytol
Pheo	2H	Phytol
Pheid	2H	H
Zn-Chld	Zn	H

Figure 1. Scheme of chlorophyll *a* structure and derivatives.

acidic media<sup>11</sup> and photostability<sup>12,13</sup> as compared to Mg-Chl (the Chl form usually found in nature). Derivatives without the phytol chain from free base chlorine and chlorophylls are the phorbides and

Received: February 8, 2011

Revised: April 29, 2011

Published: May 16, 2011

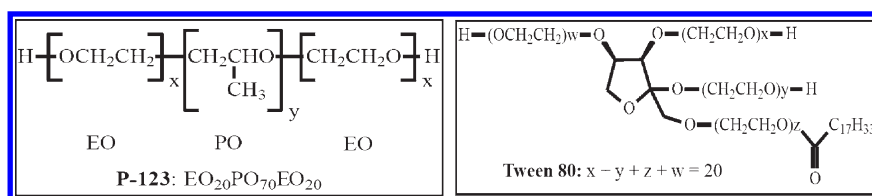


Figure 2. Structure of surfactant P-123 and Tween 80.

chlorophyllides, respectively, as evidenced by pheophorbide (Pheid) and zinc chlorophyllide (Zn-Chld) (structures presented in Figure 1).

The electronic absorption spectra of porphyrins in the visible and near UV wavelengths can be explained by the theory of the four frontier orbitals.<sup>14</sup> The Soret bands in the blue region arises from the  $S_0 - S_n$  transitions with  $n > 2$ , while the Q bands in the red region, from the  $S_0 - S_1$  and  $S_0 - S_2$  to  $Q_y$  and  $Q_x$  transitions,<sup>15,16</sup> respectively. The chlorophyll derivatives have a high molar absorptivity coefficient ( $\epsilon$ ) in the Q bands, which, allied to other characteristics such as a long lifetime of the excited state and high singlet oxygen quantum yield (unless to CuChl),<sup>13</sup> makes these compounds potentially applicable as photosensitizers in photodynamic therapy (PDT).<sup>17</sup>

The high hydrophobicity of the chlorophylls arises from the porphyrin ring, especially for free base porphyrins; the phytol chain causes aggregation in aqueous media and enhances the hydrophobicity. In plant cells, the phytol chain acts as an anchor in the positioning of chlorophyll molecules to the proper orientation in the chlorophyll–protein complexes within the chloroplasts during the process of photosynthesis. Several studies have shown the importance of the phytol chain in the interaction of Chl with hydrophobic environments and in aggregation phenomena.<sup>18–20</sup> The presence and type of metal coordinated to the porphyrin ring are also crucial for the conformation of these molecules in a given environment. Conformation changes drastically alter the properties of chlorophyll, such as generation and lifetime of excited states, directly affecting photochemical processes following light absorption.<sup>21</sup>

The complexity of natural membranes complicates the study of properties of Chl in biological tissues of animals, for instance. As the number and distribution of Chl components are highly variable, substantial study at different levels is required. Thus, model systems of simple membranes are employed, providing useful information about the properties of the molecules bound to organized systems. The micellar systems consisting of an internal hydrophobic region and a hydrophilic external aqueous solution have been used as very simple models of biological membrane interfaces.<sup>22</sup>

The use of surfactants is known to be effective in the stabilization of hydrophobic molecules in aqueous medium, such as photosensitizers monomerization. In clinical/pharmaceutical applications of polymeric surfactants is interesting to use neutral such as Tween 80 and polymers in block-type oxy-alkyl (Pluronics) due to their low toxicity compared to conventional surfactants. The balance of hydrophobicity of polymeric micelles is controlled by relative number of hydrophilic and hydrophobic monomers, resulting in the great versatility of these compounds, as can be noted from the number of copolymers commercially available for different uses in different areas, including drug solubilization and drug delivery.<sup>23</sup> Regarding the structure of the copolymer in the stabilization of hydrophobic drugs, the increase of hydrophobic blocks and the

micelle molecular weight should favor drug solubilization.<sup>24</sup> Additionally, the incorporation of drugs that have acid–base groups in polymeric micelles should be pH dependent, once their charged forms are less stabilized within the micelle and thus may be released faster than the more hydrophobic/neutral species.<sup>25</sup>

In this work, the physicochemical properties of chlorophyll *a* derivatives in homogeneous systems have been studied in terms of their acid–basic equilibrium properties, stability of metal complexes with acid treatment, and determination of the partition in the biphasic system octanol/water. Interactions of chlorophyll and its derivatives with micellar systems of neutral Tween 80 and polymeric surfactant P-123 (Figure 2) were also investigated through binding and relative localization studies.

## EXPERIMENTAL METHODS

**Samples: Chlorophyll Derivatives.** The chlorophyll *a* derivatives Mg-Chl, Zn-Chl, Cu-Chl, Pheo and Pheid were prepared according to the procedures described in the literature. Zn-Chld was generated through metalation of Pheid in a methodology similar to that used to obtain Zn-Chl from Pheo.<sup>26,27</sup>

All stock solutions ( $10^{-3}$  M) were prepared by dissolving the pure chlorophyll derivative in DMSO. The stock was standardized by absorption electronic spectroscopy in acetone (UV–vis spectrophotometer Varian, model Cary 50). The molar absorptivity coefficient ( $\epsilon$ ) values were  $\epsilon_{663\text{nm}} = 92\,600\text{ M}^{-1}\text{ cm}^{-1}$  for Mg-Chl;  $\epsilon_{667\text{nm}} = 67\,000\text{ M}^{-1}\text{ cm}^{-1}$  for Pheo;  $\epsilon_{667\text{nm}} = 56\,200\text{ M}^{-1}\text{ cm}^{-1}$  for Pheid;  $\epsilon_{656\text{nm}} = 90\,000\text{ M}^{-1}\text{ cm}^{-1}$  for Zn-Chl,  $\epsilon_{656\text{nm}} = 64\,000\text{ M}^{-1}\text{ cm}^{-1}$  for Zn-Chld; and  $\epsilon_{650\text{nm}} = 60\,000\text{ M}^{-1}\text{ cm}^{-1}$  for Cu-Chl.<sup>28–30</sup>

**Fluorescence Quantum Yield ( $\Phi_{\text{Fl}}$ ).** The  $\Phi_{\text{Fl}}$  of Chl were determined in 10% water/ethanol (v/v) solutions using Mg-Chl in ethyl ether as a standard solution,  $\Phi_{\text{Fl}} = 0.35$ .<sup>31</sup> The emission spectra were obtained with a fluorometer (Cary Eclipse, Varian). All samples presented absorbance lower than 0.05 to avoid internal filter problems. The  $\Phi_{\text{Fl}}$  was calculated by eq 1.<sup>32</sup>

$$\Phi_{\text{Fl}} = \frac{Abs_s F_c n_p^2}{Abs_c F_s n_c^2} \Phi_p \quad (1)$$

where *S* is the standard and *C* is Chl, *n* is the refractive index, and *F* is the emission spectra area. The excitation wavelength was fixed at 411 nm and the emission was registered in the range of 600–800 nm, samples at 25 °C.

Analysis of pH-dependence of Chl derivatives in homogeneous media: apparent constants of protonation ( $K_a$ ) and demetalation pH ( $\text{pH}_M$ ) investigated by electronic absorption spectroscopy.

The demetalation ( $\text{pH}_M$ ) of Chl derivatives, such as Mg-Chl, Zn-Chl, and Zn-Chld, toward the Pheo or Pheid forms, as well as the subsequent protonation of the porphyrin ring's nitrogens of the free-base porphyrins and phorbide forms ( $\text{pK}_a$ ), was investigated in homogeneous media comprised of 10% water/ethanol

(v/v) solutions. Further protonation of the carboxylic group of phorbides was also assessed.

Their  $pH_M$  and  $pK_a$  values were determined by monitoring the electronic absorption spectra of Chl ( $5 \times 10^{-6}$  M) as a function of the medium pH. The studies were performed in 10% water/ethanol solutions (v/v) in order to maintain the Chl in a monomeric state.<sup>26</sup> In this way, the pH of 10% water/ethanol (v/v) solutions in a quartz cuvette containing the Chl derivative was adjusted with the addition of small aliquots ( $\mu$ L) of acid stock solution (6 M HCl) at 30.0 °C. The titration UV–vis spectra to Chl were obtained after complete demetalation, and the  $pK_a$  and  $pH_M$  values were evaluated through statistical treatment of experimental data using principal component analysis (PCA), imbric Q-mode analysis, and the K matrix method.<sup>33</sup>

**Determination of Octanol/Water Partition Coefficient.** To a biphasic mixture containing octanol/water at 50% (v/v) was added the Chl ( $2 \times 10^{-6}$  M), and after intense stirring and 48-h rest in the dark, the Chl concentration in both phases was evaluated by UV–vis. The partition coefficient of the octanol phase ( $K_p$ ) was calculated by

$$K_p = [\text{Chl}]_o / [\text{Chl}]_w \quad (2)$$

where  $[\text{Chl}]_o$  and  $[\text{Chl}]_w$  are the molar concentrations of Chl in octanol and water, respectively.

The molar absorptivity coefficient ( $\epsilon$ ) values in  $Q_{y,0-0}$  band used were  $55\,700\text{ M}^{-1}\text{ cm}^{-1}$  for Mg-Chl;  $26\,500\text{ M}^{-1}\text{ cm}^{-1}$  for Pheo;  $30\,100\text{ M}^{-1}\text{ cm}^{-1}$  for Pheid;  $62\,100\text{ M}^{-1}\text{ cm}^{-1}$  for Zn-Chl;  $57\,100\text{ M}^{-1}\text{ cm}^{-1}$  for Zn-Chld; and  $26\,200\text{ M}^{-1}\text{ cm}^{-1}$  for Cu-Chl in water. The  $\epsilon$  values in octanol used were of  $95\,700\text{ M}^{-1}\text{ cm}^{-1}$  for Mg-Chl;  $77\,600\text{ M}^{-1}\text{ cm}^{-1}$  for Pheo;  $88\,700\text{ M}^{-1}\text{ cm}^{-1}$  for Pheid;  $93\,000\text{ M}^{-1}\text{ cm}^{-1}$  for Zn-Chl;  $87\,500\text{ M}^{-1}\text{ cm}^{-1}$  for Zn-Chld; and  $63\,000\text{ M}^{-1}\text{ cm}^{-1}$  for Cu-Chl.

**Interaction of Chl Derivatives with Micellar Microenvironments: Fluorescence Studies.** The surfactant Tween 80 [Synth, MM =  $1310\text{ g mol}^{-1}$ , critical micelle concentration (cmc) =  $1.2 \times 10^{-5}\text{ M}$ ] and the pluronic P-123 [Aldrich, MM =  $5800\text{ g mol}^{-1}$ , cmc =  $4.4 \times 10^{-6}\text{ M}$ ]<sup>23</sup> were used in the binding constant experiments and the Stern–Volmer quenching studies with the Chl. Static fluorescence emission of Chl at  $5 \times 10^{-7}\text{ M}$  was monitored in a Varian-Cary Eclipse spectrofluorometer with excitation wavelength ( $\lambda_{\text{exc}}$ ) of 411 nm. All experiments were performed at 30.0 °C.

**Binding Constants ( $K_b$ ) of Chl with Polymeric Micelles.** The binding constants ( $K_b$ ) of Chl with micelles were evaluated by the fluorescence emission spectra of Chl ( $5 \times 10^{-7}\text{ M}$ ) acquired in the presence of either P-123 or Tween 80 solutions. The amount of Chl was reduced by 10 times in comparison with UV–vis experiments in order to avoid the inner filter effect and to reduce aggregation effect. Aliquots of surfactant were added using a 2% (w/v) stock solution directly to a cuvette containing Chl in DMSO ( $[\text{DMSO}] < 0.1\%$  (v/v)) in aqueous solution. The experimental data were theoretically fitted using eq 3.<sup>34</sup>

$$F = F_0 + (F_f - F_0) / ((1/K_b([S] - \text{cmc})^N) + 1) \quad (3)$$

where  $F$  is the fluorescence emission intensity of Chl,  $F_f$  is the emission of Chl bound to the polymeric micelle,  $F_0$  is the emission of unbound Chl,  $K_b$  is the binding constant;  $[S]$ : surfactant concentration, and  $N$  is the number of surfactant molecules per molecule of Chl.

**Quenching Fluorescence Studies.** Additionally, quenching fluorescence experiments were performed with titration of Chl

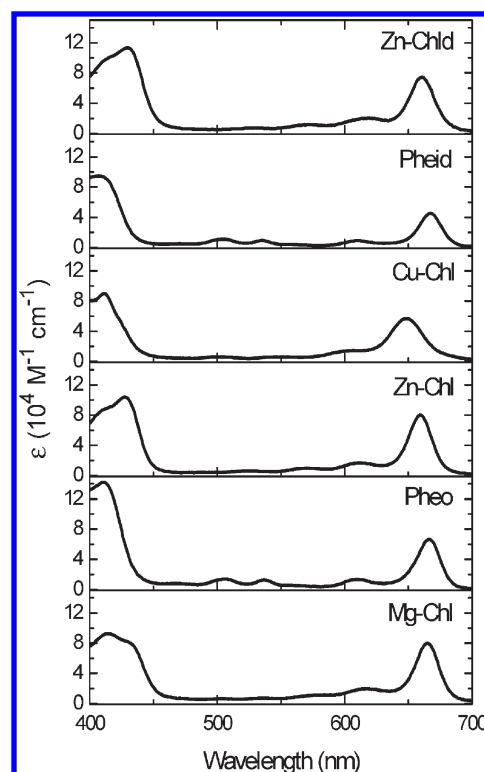


Figure 3. Electronic spectra of Chls in 10% water/ethanol, 30.0 °C.

solution ( $5 \times 10^{-7}\text{ M}$ ) in the presence of micellar systems P-123 ( $3.15 \times 10^{-4}\text{ M}$ ) and Tween 80 ( $1.5 \times 10^{-3}\text{ M}$ ), using  $\text{I}^-$  from a 3 M KI stock solution as a water-soluble quencher. Stern–Volmer constants ( $K_{SV}$ ) were calculated through<sup>35</sup>

$$F_0/F = 1 + K_{SV}[\text{I}^-] \quad (4)$$

where  $F_0$  and  $F$  are the fluorescence emission of pure Chl in solution and bound to surfactants, respectively, and  $[\text{I}^-]$  is the concentration of the iodide (quencher). The concentrations of surfactants were kept above their cmc.

## RESULTS

**Spectroscopic Properties of Chlorophyll Derivatives in Homogeneous System.** The electronic absorption spectra of Chl in 10% water/ethanol (v/v) solutions are presented in Figure 3. Two main characteristic absorption bands of chlorines can be noted, namely Soret (also known as B-band, at around 350–400 nm) and Q-band (most prominent peak at c.a. 600–660 nm). However, in the free-base compounds, Pheo and Pheid, additional weaker bands are observed in the range of 500–650 nm, arising from the asymmetry of the porphyrin ring.<sup>36</sup> Figure 3 shows that the Q-Bands of Chl complexed with  $\text{Zn}^{2+}$  and  $\text{Mg}^{2+}$  present relatively higher absorption intensities than those observed in free base forms and metalated with  $\text{Cu}^{2+}$ . On the other hand, similar to that observed in organic media,<sup>19</sup> the electronic spectra are affected only slightly by the phytol group, as observed in Pheo and Pheid, as well as in Zn-Chl and Zn-Chld, keeping the spectral profile and with changes in molar absorptivity. The wavelengths of maximum absorption ( $\lambda_{\text{abs}}$ ), molar absorption coefficients ( $\epsilon$ ), and fluorescence emission ( $\lambda_{\text{em}}$ ) from Chl spectra are shown in Table 1.



**Table 1.** Wavelengths of Maximum Absorption ( $\lambda_{\text{abs}}$ ), Molar Absorption Coefficients ( $\epsilon$ ), Fluorescence Emission ( $\lambda_{\text{em}}$ ), and Fluorescence Quantum Yield ( $\Phi_{\text{Fl}}$ ) of Chl Derivatives in 10% Water/Ethanol (v/v), at 30.0 °C

Chl	Soret		$Q_{y,0-0}$		$\Phi_{\text{Fl}}$	
	$\lambda_{\text{abs}}$ (nm)	$\epsilon$ ( $10^3 \text{ M}^{-1} \text{ cm}^{-1}$ )	$\lambda_{\text{abs}}$ (nm)	$\epsilon$ ( $10^3 \text{ M}^{-1} \text{ cm}^{-1}$ )	$\lambda_{\text{em}}$ (nm) <sup>a</sup>	( $10^{-3}$ )
Mg-Chl	430	83.1	665	79.4	667	0.5
Zn-Chl	428	103	659	80.0	663	2.1
Zn-Chld	429	11.5	660	74.2	665	16
Cu-Chl	412	90.0	650	56.0	668	~0
Pheo	411	142	667	66.7	671	6.0
Pheid	411	93.2	667	45.2	673	96

<sup>a</sup>  $\lambda_{\text{exc}} = 411 \text{ nm}$ .

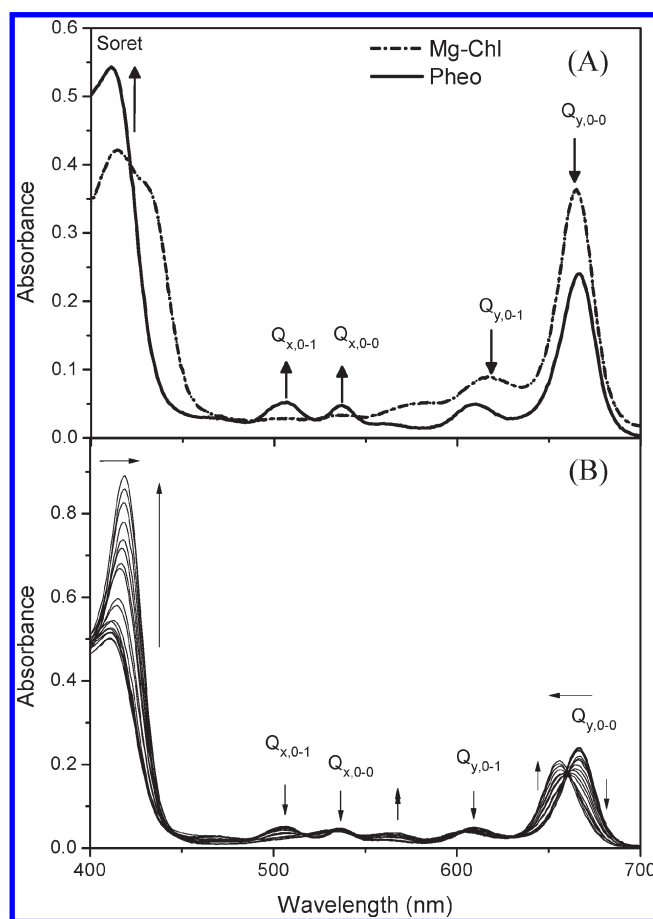
Figure 4A gives the electronic absorption spectra obtained during the Chl demetallation by acid addition in 10% water/ethanol solution, which show that the spectral properties of Chl (absorption and  $\lambda_{\text{max}}$ ) are pH-dependent. Upon acidification of the media, the demetallation effect of Mg-Chl was detected, and new species with distinct spectral features were formed. For instance, two main Q-bands, at  $\lambda_{\text{max}} = 665$  ( $Q_{y,0-0}$ ) and 615 nm ( $Q_{y,0-1}$ ), were observed initially in the Mg-Chl. Upon the reaction of demetallation and the subsequent formation of free base Pheo, the loss of symmetry of the porphyrinic ring leads to the appearance of four distinct new absorption bands.<sup>36</sup> The  $Q_{y,0-0}$  band intensity decreased in comparison with that of Mg-Chl, while a slight red shift to 667 nm was observed. Furthermore, Pheo presented a higher molar absorption coefficient with a bathochromic shift in the Soret band (Table 1 and Figure 3).

Figure 4B presents the UV-vis spectra of acid titration of free base Pheo. The spectral changes observed with Pheo protonation are again a consequence of changes in the porphyrin ring symmetry.<sup>36</sup> In this case, a hypsochromic shift and decrease of the intensity of  $Q_{y,0-0}$  band were observed in the protonated form of  $\text{Pheo}^{2+}$ , as compared to free base form of Pheo. The vibronic components  $Q_{y,0-1}$  and  $Q_{x,0-0}$  were also altered in position and intensity. For instance, the  $Q_{x,0-1}$  band at  $\lambda_{\text{max}} = 509 \text{ nm}$  disappeared (to the vibronic component of the second transition polarized along the  $x$  axis), and a significant increase of the absorption intensity of the Soret band was detected.<sup>37</sup> Similar changes in the spectra profile were also observed upon the acid titration of the Zn-Chl.

In addition, the dicationic species ( $\text{Pheo}^{2+}$  and  $\text{Pheid}^{2+}$ ) possess practically identical electronic spectra, independently of the presence or absence of the phytol chain in their structure.<sup>19</sup> Besides, the protonation of the propionate group in both phorbide compounds lead to a very slight change in their UV-vis spectra, as explored in chemometric studies (Figures 5 and 6).

**Chlorin Acid/Basic Equilibria in Homogeneous Media:  $pK_a$  and Demetallation pH ( $pH_M$ ) Determination.** As observed in Figure 4, the compounds Mg-Chl, Pheo, and  $\text{Pheo}^{2+}$  presented a remarkable spectral difference that allowed the determination of  $pH_M$  (Figure 4A), as well as of the acid equilibria constant ( $pK_{a1}$ ) of the porphyrinic ring (Figure 4B).

The electronic absorption spectra of pure species of the Chl were evaluated by chemometry (K Matrix method) and are exhibited in Figure 5A. The schematic representations of the chemical equilibria of the molecules involved in the acidification steps are presented from right to left as an insert in the same Figure 5A. In Figure 5B, the fractions calculated of each species of Mg-Chl as a function of pH are shown.

**Figure 4.** Electronic absorption spectra in 10% water/ethanol solution showing (A) the demetallation of chlorophyll (Mg-Chl) and formation of Pheo and (B) the protonation of Pheo producing  $\text{Pheo}^{2+}$ . The direction of the arrows indicates the changes in spectra with acidification of the medium (pH 9.0 down to 0.5 at 30.0 °C).

For instance, in Figure 5B, the predominance of the metalated Mg-Chl can be observed, from basic pH values down to the lowest reactional pH 3.5, at which the metal center was replaced by protons. In the pH range of 3.5 down to 1.0, the Pheo form prevailed, while at pH below 1.0, mostly the dicationic ( $\text{Pheo}^{2+}$ ) species was formed.<sup>38</sup> The same behavior was observed for Zn-Chl with the lowest  $pH_M$  found of 2.3. The values of  $pH_M$  and  $pK_a$  estimated for all derivatives are shown in Table 2.

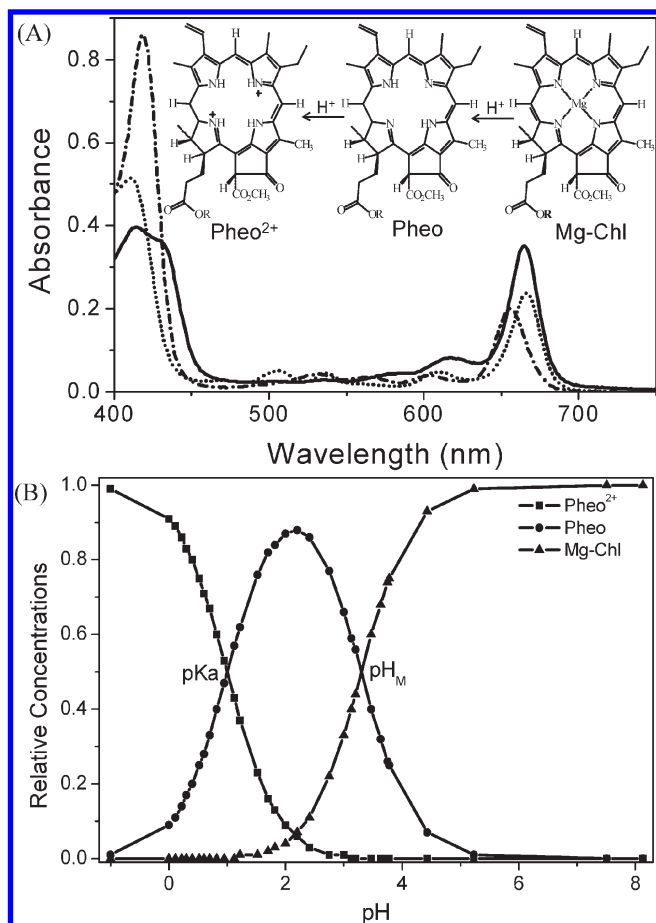


**Figure 5.** (A) Comparison of the absorption spectra of Mg-Chl, Pheo, and Pheo<sup>2+</sup> and schematic representation of the process of demetalation of chlorophyll and protonation of Pheo. Solid line, Mg-Chl; dotted line, Pheo; dashed dotted line, Pheo<sup>2+</sup>. (B) Relative concentrations of species versus pH in 10% water/ethanol solution; 30.0 °C.

For instance, the electronic absorption spectra and schematic representation of pure phorbide forms involved in acid–base equilibria of Pheid, which possesses a propionic acid group bound to C-17, are described in Figure 6A for 10% water/ethanol solutions. The anionic form Pheid<sup>−</sup> and its uncharged protonated form Pheid presented almost identical absorption spectra, whereas the equilibrium was pK<sub>a2</sub> 5.9, and again the pK<sub>a1</sub> was around 1.0 (Figure 6B).

Nevertheless, from Figure 6C, significant changes were observed in the Zn-Chld system, as well as a further distribution of species related to the metalated forms is evident. The presence of zinc shifted the pK<sub>a2</sub> value to a pH region as low as 2.4, in contrast to 5.9, as was observed for Pheid (Table 2). Moreover, the pH<sub>M</sub> estimated for Zn-Chld was 1.9, whereas the value obtained for Zn-Chl was 2.3.

The pK<sub>a1</sub> values corresponded to equilibria involving only the protonation of the porphyrin ring was around 1.0 for all systems studied, except for the system containing Cu-Chl, stable complex in acidic medium.

#### Determination of Octanol/Water Partition Coefficient.

Ensuring that the metalated structure and protolytic species remained unaltered and assuming that equilibria these systems do not change, the studies of the properties of Chl derivatives were performed in biphasic octanol/water and microheterogeneous systems (micellar solutions) and of interaction with

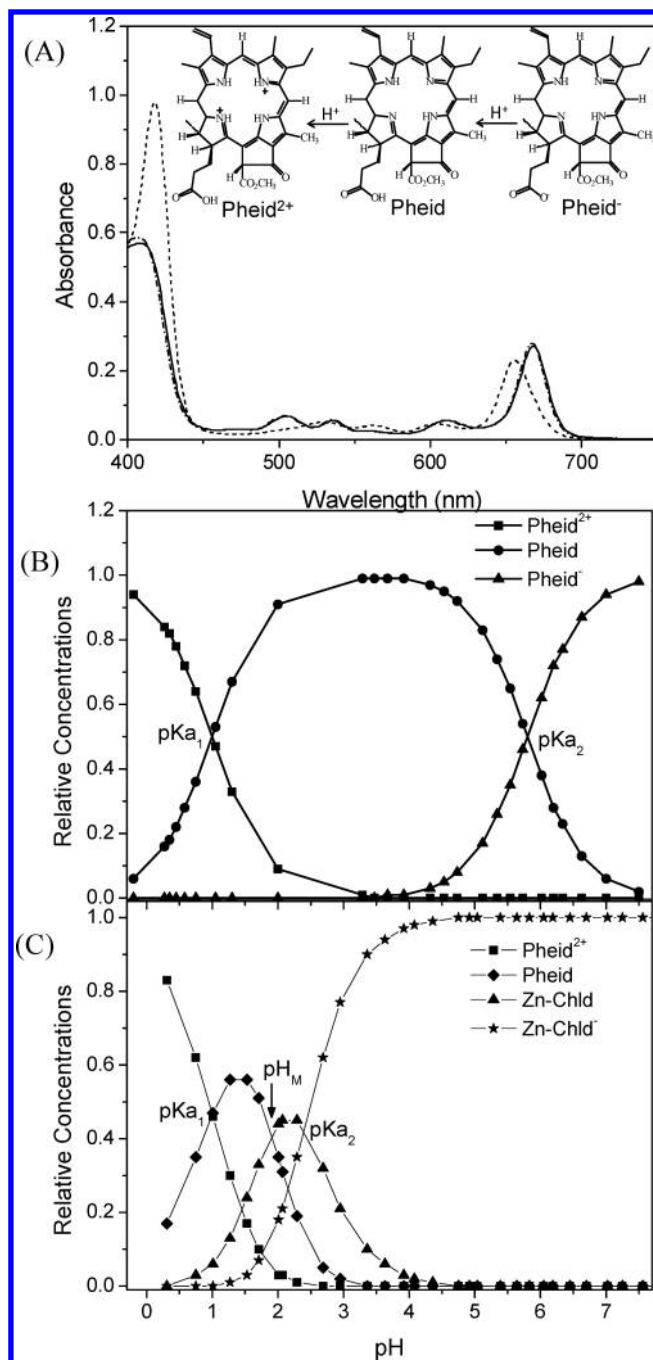


**Figure 6.** (A) Absorption spectra of species for the acid–base equilibria of Pheid with schematic representation of protonation of the carboxylic group and the nitrogens of the porphyrin ring in 10% water/ethanol solution; 30.0 °C. Solid line, Pheid; dotted line, Pheid<sup>2+</sup>; dashed dotted line, Pheid<sup>−</sup>. (B) Relative concentration of protolytic species of Pheid as a function of pH at 30.0 °C. (C) Relative concentration of protolytic species of Zn-Chld as a function of pH.

the model systems at pH ~6.0, above their pH<sub>M</sub> and pK<sub>a1</sub> values.

The values obtained for log *K<sub>P</sub>* for all Chl were greater than 0. Pheo presented the highest partition coefficient for the organic phase (*K<sub>P</sub>* = 326). Regarding the Chl with the phytol group, the *K<sub>P</sub>* observed for the compounds followed the order Pheo > Cu-Chl > Mg-Chl > Zn-Chl (Table 3), with the partition values

**Table 2.** Values of  $pK_a$  and  $pH_M$  Chlorophylls in 10% Water/Ethanol, at 30.0 °C

Chl	$pK_{a1}^a$	$pH_M^b$	$pK_{a2}^c$
Mg-Chl	1.0	3.5	
Cu-Chl			
Zn-Chl	1.1	2.3	
Zn-Chld	1.0	1.9	2.4
Pheid	1.0		5.9
Pheo	1.1		

<sup>a</sup> $pK_{a1}$ : logarithm of acid constant of the nitrogen of the porphyrin ring.  
<sup>b</sup> $pH_M$ : logarithm of hydrogen ion concentration necessary for the demetalation of the metal-porphyrin complex. <sup>c</sup> $pK_{a2}$ : logarithm of the acid constant of the carboxylic group (propionic acid residue).

**Table 3.** Octanol/Water Partition Coefficient of Chlorophylls

Chl	$K_P$	$\log K_P$
Mg-Chl	275	2.44
Zn-Chl	247	2.39
Cu-Chl	283	2.45
Zn-Chld	32	1.50
Pheo	326	2.51
Pheid	209	2.32

being somewhat similar among the chlorophylls. On the other hand, the phorbide derivatives presented smaller  $K_P$  values of 209 for Pheid, and 32 for Zn-Chld.

**Binding of Chlorophyll Derivatives in Micellar Systems: Fluorescence Studies.** The fluorescence emission spectra of Pheid ( $5 \times 10^{-7}$  M) after adding aqueous P-123 or Tween 80 solutions are illustrated in Figure 7, panels A and B, respectively. The maximum emission intensities at  $\lambda_{max} = 675$  nm as a function of surfactant concentration, presented as inserts in Figure 7, panels A and B, allowed for determining  $K_b$ .

It was observed that the emission intensity of Pheid in aqueous media was very small before the titration with surfactants (Figure 7), as observed for all the other Chl substrates, except for Zn-Chld, which is more soluble in water. Concurrently, an increase in the emission intensity was observed for all Chl with surfactant addition.

The  $K_b$  values were estimated through fitting of experimental data (inserts in Figure 7) using eq 3, shown in Table 4. Significant values of the order of  $10^4$  were obtained for the investigated derivatives, which is evidence of the meaningful interaction between Chl and the surfactants. Furthermore, the degree of association of Chl to the P-123 micellar system was higher than that of Tween 80.

The results (Table 4) showed that Zn-Chld presented the highest  $K_b$  value in both surfactants, followed by the Pheo, Cu-Chl, Mg-Chl, Zn-Chl, and finally Pheid.

The relative location of Chl in P-123 and Tween 80 micellar system was accessed by fluorescence quenching experiments using iodide anion ( $I^-$ ) as a water-soluble quencher; the Stern–Volmer plots are presented in Figure 8. Figure 8A shows that in the P-123 system Pheid and Zn-Chld were accessed by the quencher, which was evidence of a more superficial location for these substrates, thus being more exposed to  $I^-$ . This effect was also observed in micelles of Tween 80 (Figure 8B). However, in

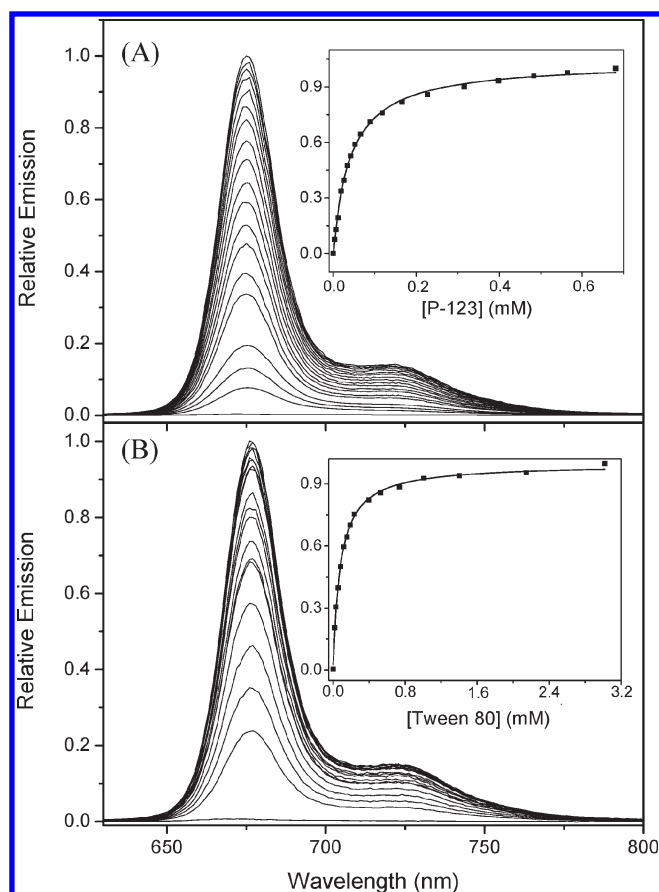


**Figure 7.** Fluorescence emission spectra of Pheid  $5 \times 10^{-7}$  M, with addition of (A) P-123 and (B) Tween 80. The inserts are related to relative emission intensities at  $\lambda_{max} = 675$  nm versus concentrations of surfactants which has been fitted by eq 3.

**Table 4.**  $K_b$  and  $K_{SV}$  of the Chlorophylls in Micellar Systems of P-123 and Tween 80, at 30.0 °C

Chl	P-123		Tween 80	
	$K_b$ ( $10^3$ M $^{-1}$ ) <sup>a</sup>	$K_{SV}$ (M $^{-1}$ )	$K_b$ ( $10^3$ M $^{-1}$ ) <sup>a</sup>	$K_{SV}$ (M $^{-1}$ )
Mg-Chl	$36.7 \pm 3.3$	0	$22.5 \pm 1.4$	$0.38 \pm 0.01$
Pheo	$51.0 \pm 1.3$	0	$41.5 \pm 3.3$	$0.39 \pm 0.01$
Zn-Chl	$28.6 \pm 1.1$	0	$19.7 \pm 1.1$	$0.57 \pm 0.02$
Cu-Chl	$37.3 \pm 1.4$	0	$25.9 \pm 1.2$	$0.40 \pm 0.05$
Pheid	$24.1 \pm 0.1$	$0.80 \pm 0.01$	$12.8 \pm 0.4$	$1.10 \pm 0.01$
Zn-Chld	$58.5 \pm 3.1$	$0.48 \pm 0.01$	$41.8 \pm 3.1$	$0.84 \pm 0.02$

<sup>a</sup>N evaluated equal 1.<sup>34</sup>

Tween 80 micelles, all Chl fluorescence emission was quenched to some extent. Table 4 shows that fluorescence quenching efficiency in Tween 80 follows the order Pheid > Zn-Chld > Zn-Chl > Cu-Chl ~ Pheo ~ Mg-Chl.

## DISCUSSION

**Spectroscopic Properties of Chlorophyll Derivatives.** Particularly for chlorines, the high  $\epsilon$  and bathochromic shift of the Q-band are suitable characteristics for PDT.<sup>39</sup> The experimental changes observed in the  $\epsilon$  and  $\lambda_{abs}$  of these absorption bands for

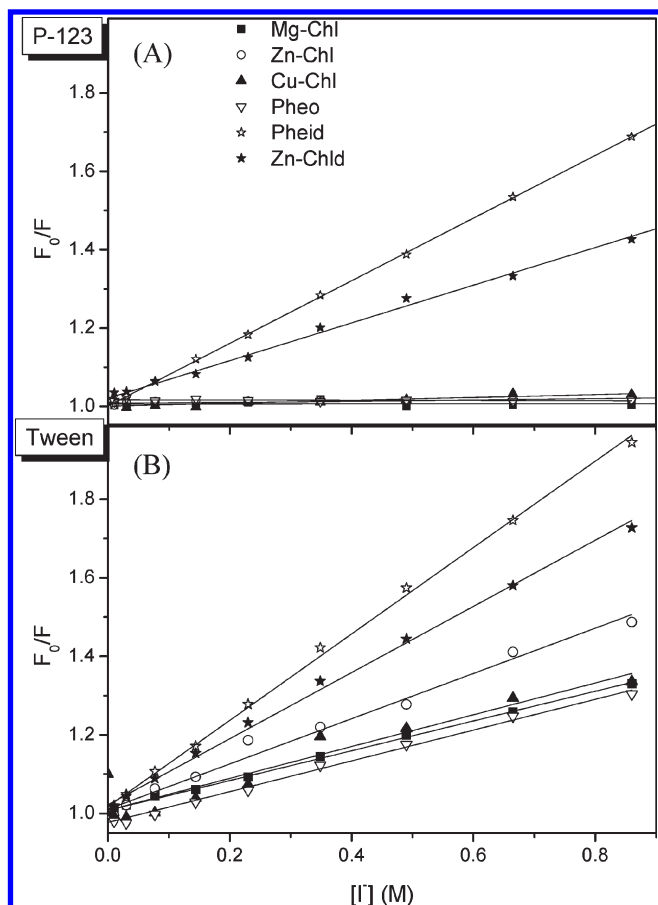


**Figure 8.** Stern–Volmer plots to chlorophyll derivatives ( $5 \times 10^{-7}$  M) with  $[I^-]$  in (A) P-123 ( $3.15 \times 10^{-4}$  M) and (B) Tween 80 ( $1.5 \times 10^{-3}$  M); 30 °C.

Chl in 10% (v/v) water/ethanol were convenient for understanding their chemical pH-dependence and photochemical properties.<sup>40</sup>

Concerning the spectral properties of Chl, the phytol chain residue affects slightly the chromophoric portion of the molecule,<sup>19</sup> which explains the spectral similarity for substrate Pheo (phytyl chain presence) with Pheid (chain absence), also observed for Zn-Chl and Zn-Chld. Similarly, this fact justifies the spectral similarity exhibited by the forms Pheid<sup>−</sup> and Pheid, Zn-Chld<sup>−</sup> and Zn-Chld that correspond to  $pK_{a2}$  equilibria. The emission properties of these derivatives are similar in shape, while the additional shoulder observed around 720 nm has been attributed to vibrational transitions.<sup>40</sup>

Unless to Cu-Chl, the acidification of chlorophyll solutions results in metal-loss compounds toward Pheo and Pheid forms. The chlorophylls with different metallic centers showed a slight bathochromic shift of the  $Q_y$ -band, as compared to the spectra of Pheo and Pheid (Table 1). These changes have been associated with the stability of the complex/ligand formed. In fact, Williams observed a bathochromic shift in a variety of metalated porphyrins in agreement with the decreasing stability of the complex,<sup>41</sup> which is also related to the electronic affinity of the metals, i.e., the reduction of the electronic conjugation of the ring.<sup>42</sup> Metalation of the free base porphyrin causes meaningful changes in its energy levels. In most cases, the porphyrinic structure can change its planar configuration dependent on metal/ligand type and

coordination state of metallic center, leading to changes in molecular symmetry from  $D_{2h}$  in symmetric system, due to the two hydrogens in opposite positions located in the ring center, to  $D_{4h}$  in which all the nitrogen atoms are equivalent.

Under subsequent protonation of these two nitrogens of tetrapyrrole ring, significant modifications of the shape and intensity of the Soret Band are noted, as well as of the number of Q bands displayed. These spectral modifications are similar to that observed when Pheo and Pheid are metalated into Chl (is the same as that observed when the free base porphyrins are submitted to protonation or metalation).<sup>36</sup> These changes affect the  $\pi$ -electron conjugation due to the protonation of nitrogen, leading to molecular symmetry modifications in the porphyrinic ring.

#### Chlorin Acid/Basic Equilibria in Homogeneous Media.

Understanding the influence of the pH on physicochemical properties of chlorophylls is important, as this may have repercussions on their stability, molecular structure, and net charge state.<sup>37</sup> Both  $pK_{a1}$  and  $pH_M$  are easy to determine due to the meaningful spectral changes observed in the involved species. However, the determination of the  $pK_{a2}$  in phorbide derivatives is difficult due to the spectral similarities, as previously discussed.

It is interesting to note the close values of  $pK_{a1}$  and  $pH_M$  of 1.1 and 2.3 for Zn-Chl and 1.0 and 1.9 for Zn-Chld, respectively. In these cases, traditional analytical treatments do not allow the unequivocal determination of  $pK_a$  because of band superposition and too close proximity of values.<sup>43</sup> However, the chemometry resulted in reliable values.<sup>44,45</sup>

The highest  $pH_M$  value found for Mg-Chl demonstrates its susceptibility to degradation in acid media, leading to Pheo formation. The value of  $pH_M$  of Zn-Chl (and Zn-Chld) was significantly lower than that of Mg-Chl, confirming its higher degree of stability.<sup>41,42</sup> Indeed, the sequence of stability of metalporphyrins has been evaluated as  $Cu^{2+} > Zn^{2+} > Mg^{2+}$ . It follows the same tendency of the Irving-Williams series, which is related to hard–soft/acid–base behavior of metal ion center,<sup>46</sup> which agrees with our results (Table 2). The  $pH_M$  of Cu-Chl was not determined, because in extreme acid conditions the chlorophyll structure degradation was observed.<sup>11</sup>

Furthermore, a dramatic decrease of  $pK_{a2}$  to 2.4 associated with the carboxylate group of Zn-Chld was observed, in comparison with the  $pK_{a2}$  of 5.9 determined for Pheid (Table 2). This meaningful difference observed between  $pK_{a2}$  Zn-Chld and Pheid can be attributed to a complex formed between the metal-porphyrin ring (electron acceptor characteristics) and the propionate group (electron donor). The propionate group presents two oxygens, which favor its complexation. In fact, the Zn coordination to the carboxylate justifies the  $pK_{a2}$  shift observed toward lower values, as the electron density in the oxygens diminished, its acidic character increased. Even after the protonation leading to the carboxylic form, one of the oxygens can remain coordinated to Zn. This interaction is weak and can also explain the smallest  $pH_M$  of Zn-Chld. This derivative presented a greater stability in acid media than its precursor Zn-Chl. The influence of the propionate group on C-17 in the axial coordination of Chl was studied by Fiedor,<sup>2</sup> who has emphasized that this group is a strong chelant agent. Usually, this kind of complexation is found in the coordination of amino acids to Zn atoms in enzymatic systems.<sup>47</sup>

Finally, the  $pK_{a1}$  values related to the nitrogens of the porphyrin ring protonation of free metal Pheo or Pheid compounds in their corresponding dicationic forms were around 1.0 for all systems. The values were shown to be independent of the residue substituent.



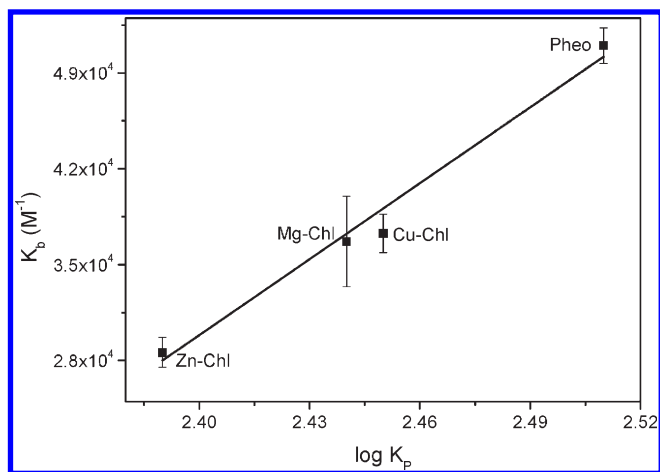


**Figure 9.** Relationship between binding constant ( $K_b$ ) and octanol/water partition coefficient ( $K_p$ ) for the CD containing phytol chain.

**Octanol/Water Partition Coefficient.** In the studies of partition coefficient constants ( $K_p$ ) of Chl in the octanol/water biphasic system,  $\log K_p$  values were greater than 0 for all derivatives, evidencing a preferential partitioning toward to the octanol phase. This fact indicates the primary tendency of Chl to incorporate into the hydrophobic microenvironment of biomembrane interfaces or membrane bilayers.<sup>48</sup>

The order estimated for  $K_p$  for the derivatives with a phytol chain was: Pheo > Cu-Chl > Mg-Chl > Zn-Chl, with similar values for the chlorophylls ( $\log K_p \approx 2.4$ ). The tendency of Pheo molecules to be partitioned into the organic phase is justified by its greater hydrophobicity in comparison with other species, such as metal-complexed ones or those without the phytol chain derivatives. The smallest values of  $K_p$  obtained for the phorbide species might be due to the replacement of the phytol chain by the propionate group (negative charge), a more water-friendly substituent.

The obtained results show the importance of the hydrophobic phytol chain of such compounds in the partitioning within hydrophobic microenvironments which should be responsible for the primary interaction of chlorophyll-proteins complexes in photosynthetic organisms.<sup>19</sup>

**Binding and Location of Chlorophyll Derivatives in Micellar Systems.** The increase in fluorescence emission of Chl as a function of surfactant concentration is associated with the presence of Chl monomers bound to micelles. All derivatives presented the  $K_b$  values in P-123 micelles higher than in Tween 80. The studies evidenced the relevance of the phytol chain on Chl structure partitioning for the octanol phase and on Chl binding to the micelles. The values of  $K_b$  for the polymeric micelles of Tween 80 and P-123 showed that substrates containing the phytol chain followed the same sequence of hydrophobicity verified through partition coefficient ( $K_p$ ) studies. The good correlation between  $K_b$  and  $K_p$  is shown through the linear relationship, as illustrated in Figure 9. It is worth mentioning that this relationship was not obeyed for the phorbide substrates. Therefore, the differences observed in  $K_b$  values are due to the hydrophobic effect, which is further modulated by the metal coordinated to the porphyrin ring in the compounds presenting the phytol chain.

The influence of the metal on the hydrophobicity scale of phytol chain-containing Chl might be explained by the ability of coordination of water molecules to the metal. For Cu-Chl, the

copper atom is tetracoordinated in planar geometry ( $d^9$  complex), as well as the free base porphyrins. Therefore, the  $Cu^{2+}$  metal usually does not provide a site for axial ligand coordination, such as water molecules.<sup>49</sup> The large  $K_p$  value observed for Cu-Chl reflects this low water affinity.

On the other hand, the pentacoordination prevails for Chl complexes with Mg and Zn that present  $d^0$  and  $d^{10}$  configurations, respectively. The pentacoordinated complexes provide a square base pyramidal geometry; however, hexacoordinated complexes of Mg-Chl are also frequent.<sup>30</sup> These complexes permit higher axial interaction/solvation by water ligands. Another factor that must be considered is the size of the metals.  $Zn^{2+}$  has a greater atomic diameter than  $Mg^{2+}$ , making the first metal leave the porphyrin plane. As a consequence, the electronegative character of Zn-Chl is enhanced, leading to high solvation by water molecules.<sup>50,51</sup> These effects explain the lowest  $K_p$  and  $K_b$  of Zn-Chl among the Chl derivatives presented in Figure 9 and Tables 3 and 4, respectively.

Furthermore, the linear relationship between  $K_b$  and  $K_p$  obtained for phytol-bound substrates contrasts with the results obtained for phorbides derivatives. One of the reasons may be the existence of distinct binding sites inside the micelle microenvironments.<sup>52</sup> Although it is expected that the Chl with phytol chain is located deeper within the micellar core due to the hydrophobic microenvironment, the Pheid probably is located in a less hydrophobic interfacial region of the micelle. However, the other phorbide compound, Zn-Chld, shows simultaneously the highest value of  $K_b$  and the lowest value of partition coefficient  $K_p$ . These results probably came from the already mentioned intramolecular complex formation between the  $Zn^{2+}$  and the propionate substituent.

Fluorescence quenching studies employing a hydrophilic iodide quencher, in which the substrate located near the aqueous interface is most sensitive, have confirmed the relative localization of Chl in the micelle. Only Pheid and Zn-Chld, were accessed by the quencher ( $I^-$ ) in the P-123 micelle system due to their greater exposure to the aqueous micellar interface. The quenching of Pheid fluorescence by  $I^-$  ( $K_{SV} = 0.80 M^{-1}$ ) was stronger than that observed for Zn-Chld ( $K_{SV} = 0.48 M^{-1}$ ). All other derivatives seem to be located deeper in the hydrophobic core of the P-123 micelle.

In the case of Tween 80, the fluorescence emission of all Chl was affected due to a greater accessibility of the quencher to the substrate, attributed to the small size of the micelle and its inability to protect large substrates within. Once again, the location of Pheid in the aqueous inner-region of the micelle was demonstrated by its highest  $K_{SV}$  values in the micelles, in agreement with its lowest  $K_b$  in Tween 80 and P-123 micelles, as well as low hydrophobic  $K_p$  parameter. The differences between Pheo and Pheid regarding their association and localization in micelles are explained by the presence of the phytol chain associated with the propionate negative charge of Pheid. The same effect was followed to Zn-Chld, however in a lesser extension. Both substrates, Pheid and Zn-Chld, exhibited the lowest partition coefficient  $K_p$  for the organic phase. The high  $K_{SV}$  value of Zn-Chld agrees with the lowest  $K_p$ , confirming the location of this substrate in a less hydrophobic region of the P-123 micelle. However, it does not justify the highest binding constant ( $K_b = 58.5 \times 10^3 M^{-1}$ ) for micelles of P-123. Apparently, Zn-Chld, which forms the intramolecular complex, firmly occupies the more hydrophilic poly(ethylene oxide) interfacial region of the P-123 micelles stabilized by hydrogen bonding interactions.

Hence, all results clearly evidenced that Pheo must be located preferentially in a deeper hydrophobic region of the micelle, carried by its pronounced hydrophobicity ( $K_p = 326$ ); this effect

was confirmed by high  $K_b$  values associated with the lowest  $K_{SV}$  among all derivatives. Despite lesser intensity, these results were followed by Cu-Chl and Mg-Chl substrates, whose locations are similar to that of Pheo in both studied micelles and also modulated by their hydrophobicity (represented by  $K_p$ ). In addition, the lowest  $K_p$  and  $K_b$  exhibited by Zn-Chl among all the investigated metalated chlorophyll containing phytyl-chain are fully consistent with the highest values of  $K_{SV}$  (in Tween 80, for instance). These results once again can be justified by their hydrophobic character.

In fact, all results involving chlorophyll substrates that present the phytyl chain can be easily explained by their hydrophobic parameter. In these cases, probably the porphyrin ring is directed toward to the aqueous interface, while the phytyl chain is maintained within the micelle internal core.

## CONCLUSIONS

Regarding the demetalation of Chl, the greater stability of Zn-Chl in acidic media in comparison to Mg-Chl was confirmed with pH studies employing chemometric methods. The  $pK_a$  found for the Pheid carboxylic group was 5.9, whereas a value of 2.4 was found for Zn-Chld, resulting from complexation of this group with the metallic center, which should also explain the weaker tendency of Zn-Chld demetalation in comparison to Zn-Chl. Besides, the apparent  $pK_a$  of nitrogens from the porphyrinic ring to their respective free base forms Pheo and Pheid was not affected, resulting in the same value of 1.0.

The partition coefficients in octanol/water biphasic systems have shown that chlorophylls preferably interact with hydrophobic moieties. The descending order of partition coefficient values was Pheo, Cu-Chl, Mg-Chl, Zn-Chl, Pheid, and Zn-Chld, according to the degree of hydrophobicity. Hydrophobicity was the key to the relative drug location in the micellar systems. All studied derivatives interacted strongly with Tween 80 and mainly with P-123 micellar systems. The role of the metallic center in Chl with bound phytyl-chain was evidenced through correlation between  $K_b$  and  $K_p$  values and explained by the ability of water coordination to the metals. For both surfactants, the order followed by  $K_b$  was Zn-Chld > Pheo > Cu-Chl > Mg-Chl > Zn-Chl > Pheid. Fluorescence quenching studies have shown that the phorbide derivatives are located in a less hydrophobic interfacial region than the phytyl-bound chain derivatives, which are located preferentially in a deeper hydrophobic micellar microenvironment. Thus, the association of the Chl with specific binding sites of micellar systems is strongly modulated by the presence of the phytyl chain and the metal coordinated to the porphyrinic ring.

## AUTHOR INFORMATION

### Corresponding Author

\*E-mail: wcaetano@uem.br. Telephone: +55-44-3011-3665. Fax: +55-44-3011-4125.

## ACKNOWLEDGMENT

This work was supported by the Brazilian granting agencies Fundação Araucária/Paraná, CNPq, and CAPES/NanoBiotec.

## REFERENCES

- (1) Krause, G. H.; Weis, E. *Annu. Rev. Plant Physiol. Plant Mol. Biol.* **1991**, *42*, 313–349.
- (2) Fiedor, L.; Kania, A.; Myśliwa-Kurczel, B.; Orzeł, L.; Stochel, G. *Biochim. Biophys. Acta* **2008**, *1777*, 1491–1500.
- (3) Fenna, R. E.; Matthews, B. W. *Nature* **1975**, *258*, 573–577.
- (4) Katz, J. J.; Shipman, L. L.; Cotton, T. M.; Janson, T. J. Chlorophyll aggregation: coordination interactions in chlorophyll monomers, dimers, and oligomers. In *The Porphyrins*; Academic Press: New York, 1978; Vol. 5.
- (5) Eccles, J.; Honig, B. *Proc. Natl. Acad. Sci. U.S.A.* **1983**, *80*, 4959–4962.
- (6) Scherz, A.; Parson, W. W. *Biochim. Biophys. Acta* **1984**, *766*, 666–678.
- (7) Spiedel, D.; Roszak, A. W.; McKendrick, K.; McAuley, K. E.; Fyfe, P. K.; Nabedryk, E.; Breton, J.; Robert, B.; Cogdell, R. J.; Isaacs, N. W.; Jones, M. R. *Biochim. Biophys. Acta* **2002**, *1554*, 75–93.
- (8) Hooper, J. K.; Eggink, L. L.; Chen, M. *Photosynth. Res.* **2007**, *94*, 387–400.
- (9) Brotsudarmo, T. H. P.; Mackowski, S.; Hofmann, E.; Hiller, R. G.; Braüchle, C.; Scheer, H. *Photosynth. Res.* **2008**, *95*, 247–252.
- (10) Fennema, O. R. *Química de los Alimentos*; Acirbia: Zaragoza, 2000.
- (11) Dujardin, E.; Laszio, P.; Sacks, D. J. *Chem. Educ.* **2003**, *52*, 742–744.
- (12) Limantara, L.; Koehler, P.; Wilhelm, B.; Porra, R. J.; Scheer, H. *Photochem. Photobiol.* **2006**, *82*, 770–780.
- (13) Gerola, A. P.; Santana, A.; França, P. B.; Tsubone, T. M.; Oliveira, H. P. M.; Caetano, W.; Kimura, E.; Hioka, N. *Photochem. Photobiol.* "Accepted Article"; doi: 10.1111/j.1751-1097.2011.00935.x.
- (14) Gouterman, M. *J. Mol. Spectrosc.* **1961**, *6*, 138–163.
- (15) Weiss, C. Optical spectra of chlorophylls. In *The Porphyrins*, Physical Chemistry. Part A; Academic Press: New York, 1978; Vol. 3.
- (16) Shipman, L. L.; Cotton, T. M.; Norris, J. R.; Katz, J. J. *J. Am. Chem. Soc.* **1976**, *8*, 8222–8230.
- (17) Brandis, A. S.; Salomon, Y.; Scherz, A. Chlorophyll Sensitizers in Photodynamic Therapy. In *Chlorophylls and Bacteriochlorophylls*; Springer: IL, 2006.
- (18) Proll, S.; Wilhelm, B.; Robert, B.; Scheer, H. *Biochim. Biophys. Acta* **2006**, *1757*, 750–763.
- (19) Fiedor, L.; Stasiek, M.; Mysliwa-Kurczel, B.; Strzalka, K. *Photosynth. Res.* **2003**, *78*, 47–57.
- (20) Agostiano, A.; Catucci, L.; Colofemmina, G.; Della Monica, M.; Scheer, H. *Biophys. Chem.* **2000**, *84*, 189–194.
- (21) Angerhofer, R. Chlorophyll Triplets and Radical Pairs. In *Chlorophylls*; CRC Press: London, 1991.
- (22) Fendler, J. H. *Membrane Mimetic Chemistry*; John Wiley & Sons: New York, 1982.
- (23) Kabanov, A. V.; Zhu, J. Pluronic Block Copolymers for Drug and Gene Delivery. In *Polymeric Drug Delivery Systems*; Kwon, G. S., Ed.; Taylor & Francis Group: Boca Raton, FL, 2005; pp 577–613.
- (24) Torchilin, V. P. *J. Controlled Release* **2001**, *73*, 137–172.
- (25) Tong, W. Q.; Wen, H. Preformulation Aspects of Insoluble Compounds. In: *Water-Insoluble Drug Formulation*, 2nd ed.; Liu, R., Ed.; Taylor & Francis Group: Boca Raton, FL, 2008; pp 61–90.
- (26) Moreira, L. M.; Lima, A.; Soares, R. R. S.; Batistela, V. R.; Gerola, A. P.; Hioka, N.; Bonancin, J.; Severino, D.; Baptista, M. S.; Machado, A. E. H.; Rodrigues, M. R.; Codognoto, L.; Oliveira, H. P. M. *J. Braz. Chem. Soc.* **2009**, *20*, 1653–1658.
- (27) Hynninen, P. H.; Löjtömen, S. *Synthesis* **1980**, 539–541.
- (28) Kupper, H.; Spiller, M.; Küpper, F. C. *Anal. Biochem.* **2000**, *286*, 247–256.
- (29) Wasielewski, M. R.; Svec, W. A. *J. Org. Chem.* **1980**, *45*, 1969–1974.
- (30) Dolphin, D. The porphyrins. *Physical Chemistry. Part A*; Academic Press Inc.: New York, 1978; Vol. 3.
- (31) Nyman, E. S.; Hynninen, P. H. *J. Photochem. Photobiol. B: Biol.* **2004**, *73*, 1–28.
- (32) Valeur, B. *Molecular Fluorescence: Principles and Applications*; Wiley: Weinheim, Germany, 2002.
- (33) Março, P. H.; Scarminio, I. S. *Anal. Chim. Acta* **2007**, *583*, 138–146.

- (34) Caetano, W.; Tabak, M. *Spectrochim. Acta, Part A* **1999**, 55, 2513–2528.
- (35) Lakowicz, J. R. *Principles of Fluorescence Spectroscopy*, 3rd ed.; Springer: New York, 2006.
- (36) Gurinovich, G. P.; Sevchenko, A. N.; Solovev, K. N. *Soviet Phys. Uspekhi* **1963**, 6, 67–105.
- (37) Hynninen, P. H. *J. Chem. Soc., Perkin Trans.* **1991**, 2, 669–678.
- (38) Tessaro, A. L.; Fernandes, D. M.; Terezo, A. J.; Souza, V. R.; Hioka, N. *J. Porphyrins Phthalocyanines* **2005**, 9, 609–616.
- (39) Sternberg, E. D.; Dolphin, D. *Tetrahedron* **1998**, 54, 4151–4202.
- (40) Horton, P.; Ruban, A. V.; Walters, R. G. *Annu. Rev. Plant Physiol. Plant Mol. Biol.* **1996**, 47, 655–658.
- (41) Williams, R. J. P. *Chem. Rev.* **1956**, 56, 299–328.
- (42) Drzewiecka-Matuszek, A.; Skalna, A.; Karocki, A.; Stochel, G.; Fiedor, L. *J. Biol. Inorg. Chem.* **2005**, 10, 453–462.
- (43) Batistela, V. R.; Cedran, J. C.; Oliveira, H. P. M.; Scarminio, I. S.; Ueno, L. T.; Machado, A. E. H.; Hioka, N. *Dyes Pigm.* **2010**, 86, 15–24.
- (44) Sena, M. M.; Scarminio, I. S.; Collins, K. E.; Collins, C. H. *Talanta* **2000**, 53, 453–461.
- (45) Gholivand, M. B.; Ghasemi, J. B.; Saaipour, S.; Mohajeri, A. *Spectrochim. Acta, Part A* **2008**, 71, 1158–1165.
- (46) Phillips, J. N. *Comprehensive Biochemistry*; Elsevier Publishing Co.: Amsterdam, 1963.
- (47) Bertini, I.; Luchinat, C.; Monnanni, R. *J. Chem. Educ.* **1985**, 62, 924–927.
- (48) Smith, D.; Waterbeemd, H.; Walker, D.; Mannhold, R.; Kubinyi, H.; Timmerman, H. *Pharmacokinetics and Metabolism in Drug Design*; Wiley-VCH Verlag: Weinheim, Germany, 2001.
- (49) Fujiwara, M.; Tasumi, M. *J. Phys. Chem.* **1986**, 90, 250–255.
- (50) Timkovick, R.; Tulinsky, A. *J. Am. Chem. Soc.* **1969**, 91, 4430–4432.
- (51) Nonomura, Y.; Igarashi, S.; Yoshioka, N.; Inoue, H. *Chem. Phys.* **1997**, 220, 155–166.
- (52) Kepczynski, M. R.; Pandian, P.; Smith, K. M.; Ehrenberg, B. *Photochem. Photobiol.* **2002**, 76, 127–134.